ELSEVIER

Journal of Hazardous Materials 52 (1997) 265–286

JOURNAL OF HAZARDOUS MATERIALS

Long-term behavior of a portland cement–electroplating sludge waste form in presence of copper nitrate

Amitava Roy *, Frank K. Cartledge

Institute for Recyclable Materials and Department of Chemistry, Louisiana State University, Baton Rouge, LA 70803, USA

Abstract

The microchemistry and microstructure of a waste form containing a synthetic electroplating sludge in portland cement (OPC) in the presence of various amounts (2%, 5%, and 8%) of copper nitrate were studied over a period of eight years. The electroplating sludge, dewatered to 25% solids, contained 86.2 mg g^{-1} of Ni, 84.1 mg g^{-1} of Cr, 18.8 mg g^{-1} of Cd, and 0.137 mg g^{-1} of Hg. The OPC to sludge ratio was 0.3:1. A waste form without copper nitrate was prepared as control. The microstructure and microchemistry were studied by scanning electron microscopy, energy dispersive X-ray spectrometry, X-ray diffractometry, thermal analysis and Fourier-transform infrared spectroscopy. Increasing amounts of copper nitrate effected significant changes in crystallinity, porosity and phase chemistry. The principal copper-bearing phase in the presence of copper nitrate was $CuO \cdot 3H_2O$, whose appearance was both time- and concentration-dependent. Some amount of copper was also trapped in the newly formed crystalline calcium silicates. At the same copper nitrate level, subtle changes in the microchemistry occurred over time, but the microstructure remained qualitatively unchanged. Some of the sludge heavy metal phases disappeared with increasing copper nitrate concentration but others were not affected. © 1997 Elsevier Science B.V.

Keywords: Copper nitrate; Long-term behaviour; Electroplating sludge; Solidification/stablization

1. Introduction

Solidification/stabilization (S/S) of hazardous waste as a process for ultimate disposal is a mature technology [1]. Though S/S has been practiced for the last four

* Corresponding author. E-mail: Reroy@unix1.sncc.lsu.edu.

PII S0304-3894(96)01812-2

Table 1
Sample preparation scheme [a]

Binder	Portland Cement
Sludge	Ni: 86.2 mg g^{-1}, Cr: 84.1 mg g^{-1}, Cd: 18.8 mg g^{-1}, Hg: 0.137 mg g^{-1}. The sludge was dewatered to 25% solids. Hydroxides of the heavy metals were precipitated by the addition of CH to a solution containing their nitrate species.
Binder/Sludge Ratio	0.3:1 OPC:Sludge
Interference (copper nitrate, $Cu(NO_3)\cdot 3H_2O$)	0, 2, 5 and 8 wt%.

[a] see [4] and [5] for details of sample preparation.

decades, the scientific basis of the process is still incompletely understood. The leachability of waste species in a particular waste form will depend on the nature of the waste chemical species present and their solubility in the percolating groundwater. The long-term performance of solidified/stabilized waste forms has been hard to predict because very little is known about waste chemical species in waste forms and their behavior over time. If a waste is present as a metastable species, it may change over the long-term into more stable species and its solubilities will also change.

There have been few studies on the long-term behavior of waste forms. For example, Perry et al. [2] studied the leachability of waste forms containing various heavy metal wastes stabilized by different vendors. They found that leachability was waste-specific, and to a lesser extent, binder-specific. With time, the leaching rate decreased for certain types of waste but increased for some other kinds of waste. Akhter and Cartledge [3] [1] studied the effect of arsenic on the cementitious matrix used for S/S by ^{29}Si and ^{27}Al magic angle spinning nuclear magnetic resonance spectroscopy. Changes in the matrix (poorly crystalline calcium silicate hydrate) structure were observed, even after one year. These studies, however, did not identify the chemical species present in the waste form.

The microchemistry and microstructures of an eight-year old portland cement and a synthetic electroplating sludge waste form in the presence of copper nitrate were investigated in this study. Such a waste form occurs during S/S of the waste generated by electroplating operation. The objectives of the study are: (i) identify the waste chemical species in the waste form; (ii) characterize the effects of copper nitrate (which is acidic) on the S/S process, copper nitrate being a compound which can interfere with the hydration process of OPC and (iii) evaluate the long-term behavior of the waste form.

The synthetic electroplating waste consists of Ni, Cr, Cd and Hg [4]. The sample preparation scheme is briefly shown in Table 1. The details of sample preparation, the specimen unconfined compressive strengths and the results of the EP toxicity test are provided elsewhere [4,5]. The properties of the waste form were monitored periodically since its preparation by several analytical techniques. The analytical techniques are scanning electron microscopy, energy-dispersive X-ray spectrometry, X-ray diffractome-

[1] See also companion paper in this issue.

try, thermal analysis, and Fourier-transform infrared spectroscopy. Taylor Eighmy et al. [6] have recently used a similar multi-technique approach to characterize element speciation and leaching behavior of municipal waste incineration electrostatic precipitator ash.

The nature of the sludge has been discussed in detail by Roy et al. [7], and was found to be a mixture of complex hydroxides and hydrated phases of the heavy metals.

2. Experimental

Over the years, the samples were stored in polyethylene bottles. The individual pieces of the solidified/stabilized samples, usually one to two inches in diameter, were dry. No changes in physical characteristics of the samples were observed with the naked eye over this period of time. For X-ray diffractometry, thermal analysis and infrared spectroscopy the samples were ground with an agate mortar and a pestle and, if possible, passed through a 200-mesh sieve. While grinding samples for XRD or thermal analysis, the samples with 8% copper nitrate and sludge were found to be very moist compared to the samples containing lower levels of copper nitrate or only sludge. The sample of portland cement was granular instead of being a larger monolith, because of the high water/solids (2.5) ratio.

2.1. Scanning electron microscopy and energy dispersive X-ray micro-analysis (SEM and EDXRA)

Scanning electron microscopy was performed with Cambridgescan S-260 and JEOL 840 microscopes. The operating voltage was usually 20 keV. The JEOL 840 was fitted with a Tracor Northern energy-dispersive X-ray spectrometer for X-ray micro-analysis. The dimensions of some the particles analyzed by EDXRA were often close to the resolution of the electron beam (diameter ca. 1 μm). Efforts were made in those instances to center the beam in the middle of a cluster of such particles so that the characteristic X-rays were generated solely from the same phase. The photomicrographs accompanying the EDXRA analyses were recorded digitally.

2.2. X-ray diffractometry (XRD)

XRD runs of four-year old and eight-year old samples were conducted with a Scintag Pad-V automated diffractometer. The samples were run from 3° to 70° 2θ at a step width of 0.02° and a counting time of at least 3 s. Cu Kα radiation was used and the excitation conditions were 45 keV and 35 mA current. The four-month old sample runs were made with a Rigaku diffractometer over the same 2θ range and same step-width but with a micro-focusing X-ray tube whose excitation conditions were 40 keV and 30 mA.

2.3. Thermal analysis

2.3.1. Differential scanning calorimetry (DSC)

The DSC runs were conducted with a Seiko TA 220 Differential Scanning Calorimeter. The samples were run from 40 to 525°C at a rate of 5°C min^{-1} in a nitrogen atmosphere. Alumina was used as standard.

2.3.2. Thermogravimetry and derivative thermogravimetry (TG and DTG)

The thermogravimetric runs were made from 25 to 1000°C with the following steps: (i) 25 to 40°C at 5°C min^{-1}; held for 10 min at 40°C; 40 to 200°C at 5°C min^{-1}; and 200 to 1000°C at 10°C min^{-1}, using a Seiko TA 220 thermal analyzer. Nitrogen was used as the purge gas. The samples were not oven-dried or otherwise treated because trial runs suggested that AFt and other hydrated phases will decompose by 105°C. The samples were analyzed immediately after grinding. The amount of sample ranged from 15 to 25 mg. The weights of CH (cement chemist's notation: $A = Al_2O_3$; $C = CaO$; $F = FeO$; $H = H_2O$; $S = SiO_2$; $C^- = CO_2$; $\bar{S} = SO_3$), AFt (alumino–ferrite trisulfate or ettringite) and CC^- obtained from derivative thermogravimetry (DTG) are normalized to the weight of the sample at 40°C, where it was held for 10 min to remove the moisture. The peak areas were determined using Peakfit™ from Jandel Scientific Software.

A chemical compound containing several molecules of water usually loses the molecular water in several steps, over a temperature range. At a high heating rate, these steps will overlap, but a slower heating rate can resolve (at least partially) these peaks. In order to resolve the peaks in the 200 to 400°C range better, the samples were also run at a slower heating rate (3°C min^{-1}) over the range. Though the resolution was better, no new peaks were revealed.

2.4. Fourier-transform infrared spectroscopy (FTIR)

Fourier-transform infrared spectroscopy was performed with a Perkin Elmer 1700 series spectrometer equipped with a TGS (triglycine sulfate) detector. Optically transparent discs were prepared in the mini-press from powdered samples mixed with KBr. The samples were dried at 50°C for several hours before KBr discs were made. The scanning range was from 4000 to 400 cm^{-1}, and the number of scans averaged were, at the minimum, 5 at a scan speed of 0.4 cm s^{-1} and resolution of 4 cm^{-1}.

3. Results

In this section only data from the eight-year old waste forms are considered, unless specified otherwise.

3.1. Sludge

The DSC curve of the sludge is shown in Fig. 1. Apart from the CH peak around 466°C, several peaks were present in the curve: at 103, 272 and 323°C. A weak shoulder

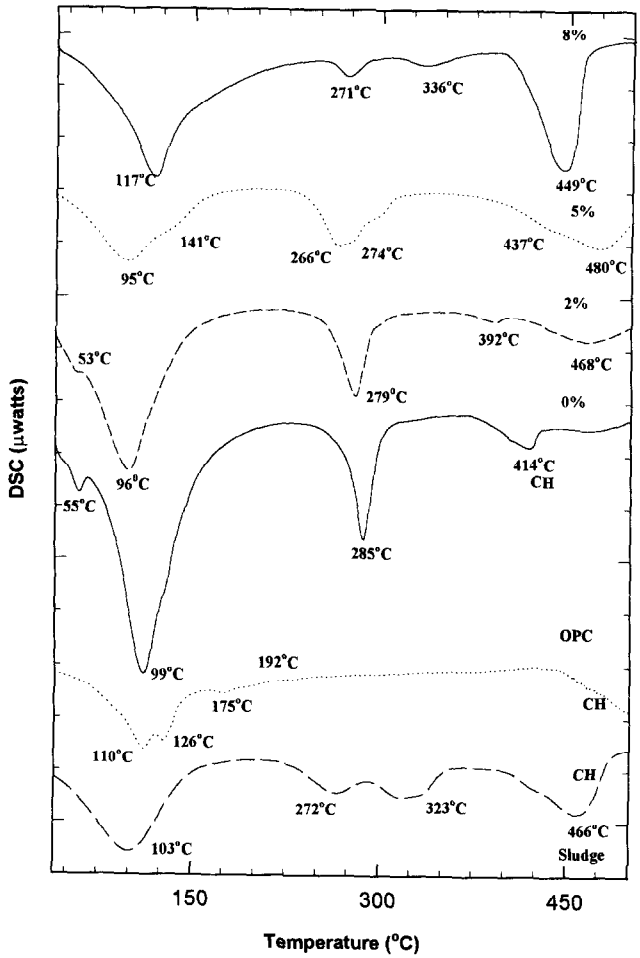

Fig. 1. DSC curves of OPC–sludge–copper nitrate waste form, along with that of the sludge, are shown.

was also present on the 466°C peak. The DTG curve of the sludge is shown in Fig. 2. In the region 200 to 500°C, the curve consisted of several partially resolved peaks. A comparison to the pure CH and CC^- curves suggests that the peaks at 426 and 723°C were due to CH and CC^-, respectively. The amount of CC^- in the sludge was high (35%). The granular nature of the waste form, with its attendant high porosity, made it highly susceptible to carbonation. The FTIR spectrum of the sludge (Fig. 3 and Table 2) shows that the H_2O peak was strong and the OH peak was also significant. The peaks in the DSC and DTG curves of sludge were then due to the loss of molecular water, hydroxyl molecules and carbon dioxide from the heavy metal species, lime, and carbonated lime.

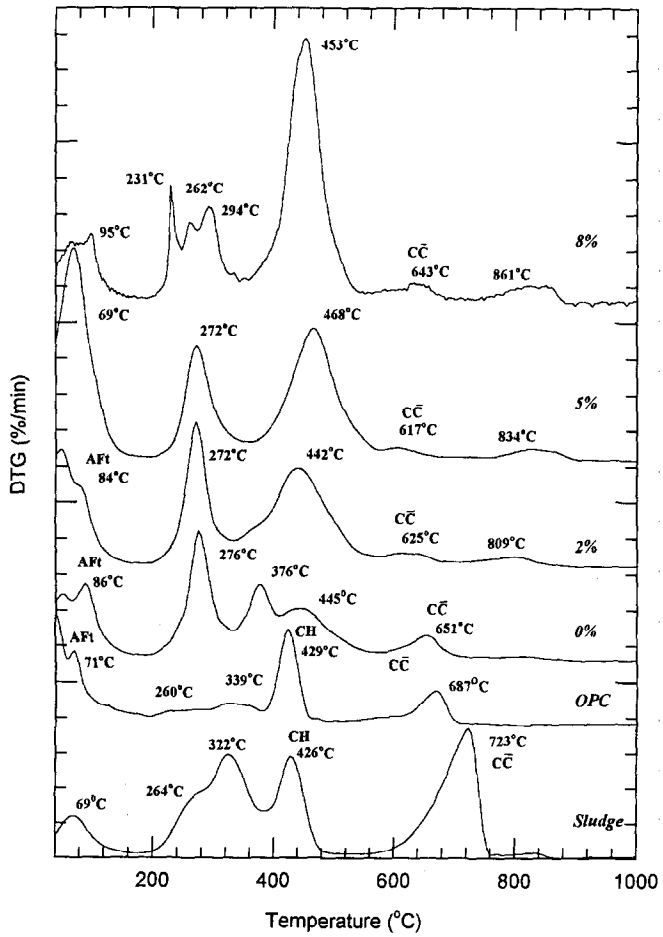

Fig. 2. DTG curves of OPC–sludge–copper nitrate waste form, along with that of the sludge, are shown.

3.2. Portland cement-sludge-copper nitrate waste form

3.2.1. Scanning electron microscopy

Thin irregularly-shaped plates, a few micrometers in diameter, constituted the matrix of the OPC–sludge waste form [7]. These platelets were sometimes present as spherules, ca. 10 μm in diameter. Dense, spherical grains, ca. 30 to 40 μm long, were commonly found embedded in the matrix of the waste form. These were composed of irregular sub-micrometer-size platy grains, arranged tangentially to the surface. In contrast to these spherical grains, the matrix was more porous.

The addition of 2% copper nitrate to the waste form led to the appearance of several newer morphologies. One was roughly equidimensional, often as much as 40 μm in diameter, with smooth faces. The second type was elongated crystals bounded by very well developed orthorhombic prismatic and domal faces, and up to 5 to 6 μm in length,

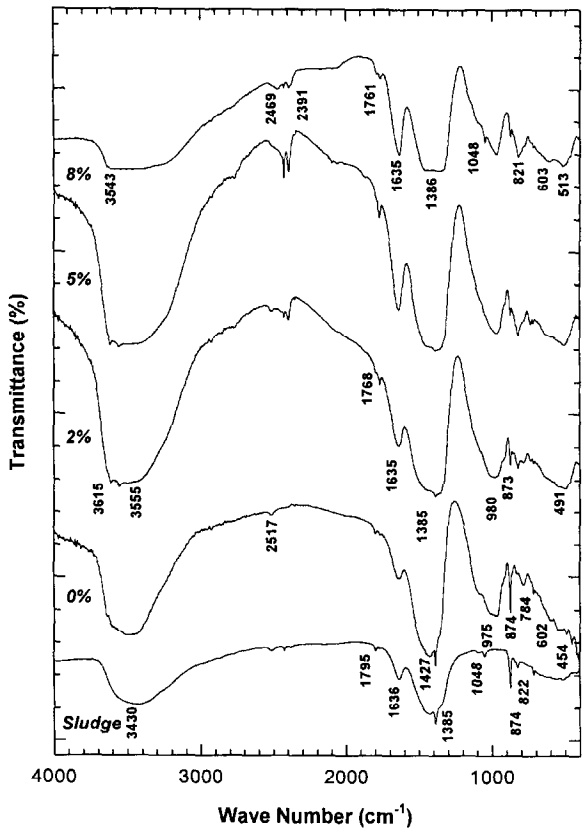

Fig. 3. FTIR patterns of OPC–sludge–copper nitrate waste form, along with that of the sludge, are shown.

identical to those shown in Fig. 4. Both of these morphologies were distinctly different from the surrounding ill-defined plates, which constituted the bulk of the waste form. However, the faces of the matrix phase were better developed, compared to the control sample.

In the presence of 5% copper nitrate, a new phase with a thin fiber-like morphology appeared. The crystals were usually present in parallel bunches or radiating fibers. The prismatic crystals with domal faces were also present at the 5% copper nitrate level. The dense sludge particles were also common.

The change in matrix morphology was most conspicuous at 8% copper nitrate level. A crystalline phase with prismatic and pyramidal faces, as much as 6 μm in length, was extremely common. Even at a few hundred times magnification, these crystals appeared to make up a significant portion of the waste form (Fig. 5). The sludge particles, the morphology with orthorhombic and prismatic faces, were all present at 8% copper nitrate level.

The addition of the sludge and copper nitrate brought distinct changes to the microstructure of OPC. Massive CH crystals are very common in OPC, particularly in

Table 2
Partial list of peaks in OPC-sudge-copper nitrate waste form (in nm)

0%	2%	5%	8%	Comments
	1.037	1.032		
			0.981	
0.868				Sludge
		0.803	0.808	Sludge
0.798	0.798			Sludge
			0.709	
	0.649	0.647	0.650	$CuO \cdot 3H_2O$
		0.582	0.584	
			0.564	
		0.513		
			0.499	Sludge
	0.473	0.470	0.473	Sludge; $CuO \cdot 3H_2O$
			0.451	
			0.442	
0.432	0.433			Sludge
			0.424	$CuO \cdot 3H_2O$
				Sludgde
0.399	0.400	0.402	0.403	Sludge
0.397				
			0.364	Sludge
		0.392		
		0.343		$CuO \cdot 3H_2O$
	0.324	0.322	0.325	Sludge
0.300	0.300	0.301	0.300	
0.292	0.292	0.291	0.292	Sludge
0.288				
	0.284	0.283		$CuO \cdot 3H_2O$
0.276	0.276		0.277	Sludge
			0.269	
			0.266	Sludge
	0.262			$CuO \cdot 3H_2O$
	0.259	0.258	0.259	
0.255				
	0.243		0.244	
0.241	0.241			Sludge
	0.236	0.236	0.236	$CuO \cdot 3H_2O$
			0.231	Sludge
	0.223			
			0.214	Sludge
			0.210	Sludge
		0.208		
	0.195		0.197	
			0.185	
	0.181	0.181		
	0.180			
			0.176	
	0.173			

Table 2 (continued)

0%	2%	5%	8%	Comments
	0.169	0.168	0.169	$CuO \cdot 3H_2O$
	0.167		0.166	
	0.152			
			0.146	
		0.142		

Fig. 4. Scanning electron photomicrograph of a 4-month-old OPC–sludge waste form sample with 8% copper nitrate. The bar scale on top left is 1 μm.

Fig. 5. Scanning electron photomicrograph of an OPC sample with sludge and 8% copper nitrate.

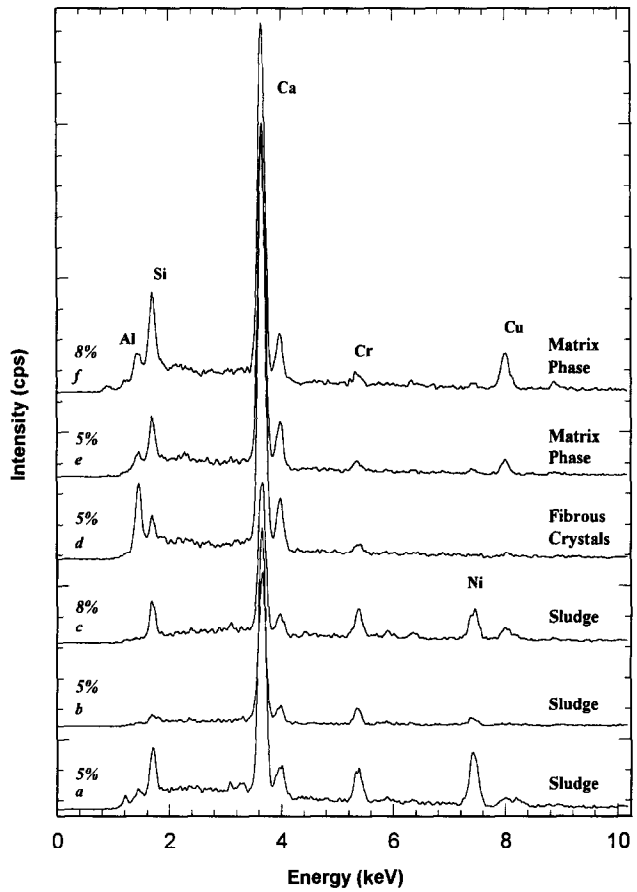

Fig. 6. EDX spectra of some phases in OPC–sludge–copper nitrate waste form.

mature cement paste. Such crystals were completely absent in the waste form. Distinct particles of sludge were always present, irrespective of copper nitrate concentration. The porosity increased gradually with increasing copper nitrate concentration, most of which was in between the plate-like phase in the matrix.

3.2.2. Energy dispersive X-ray micro-analysis

Some representative EDXRA spectra are shown in Fig. 6. The first three analyses were of the spherical sludge particles (Fig. 7a) in the 5% and 8% copper nitrate containing waste form. Ca, Cr and Ni were the principal elements in various proportions. One analysis had a significant amount of Si, whereas another analysis was completely devoid of it. Cu was absent in all these analyses.

Fig. 2d shows the analysis of the crystals with thin fiber-like morphology disposed in radiating fashion (Fig. 7b). Fig. 6e represents an analysis of the plate-like matrix phase in the 5% copper nitrate containing waste form (Fig. 7c). An analysis of the matrix

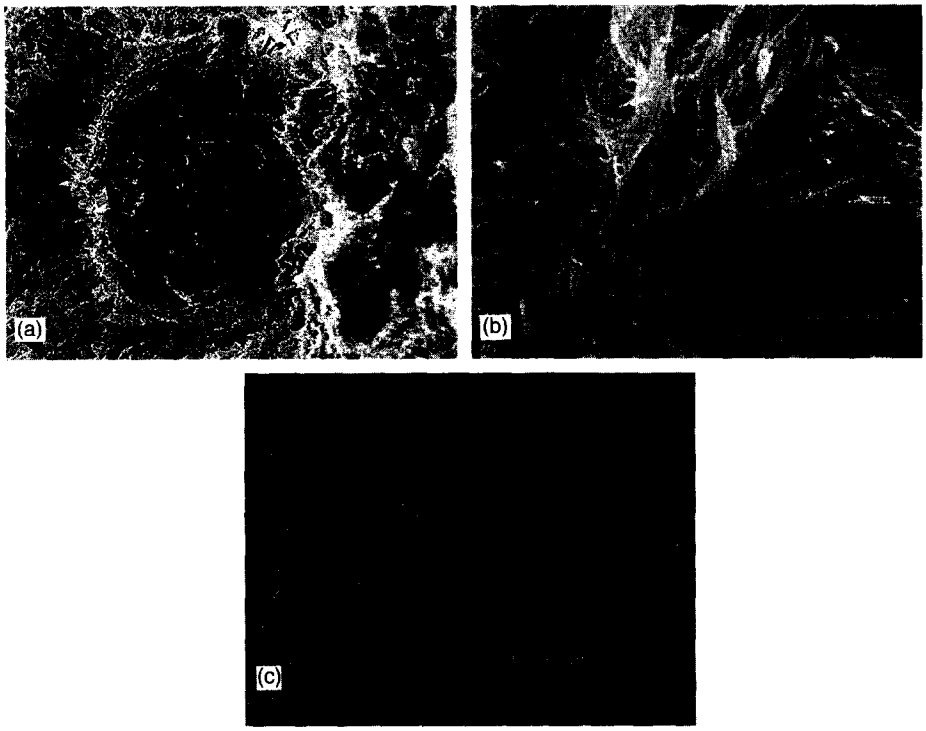

Fig. 7. Scanning electron photomicrographs of phases analyzed by EDXRA; (a) sludge particle in 8% copper nitrate-containing waste form; (b) fibrous crystals in 5% copper nitrate-containing waste form; (c) plate-like phase in the matrix of 5% copper nitrate-containing waste form.

phase from the 8% copper nitrate waste form (Fig. 5) is shown in Fig. 6f. All these phases were alumino–silicates, incorporating variable amounts of Cr and Cu.

3.2.3. X-ray diffractometry

Fig. 8 shows the XRD patterns of the waste form with increasing amounts of copper nitrate, and a partial list of the peaks in the waste form is given in Table 3. The peaks for AFt, CH and CC^-, which were present in some cases as discussed below, are not listed in the Table.

The OPC–sludge waste form contained appreciable amounts of CH and Aft, the two principal hydration products of OPC. Some amounts of CC^- was also detected. Peaks such as the 0.868, 0.798, 0.473, 0.399, 0.292 nm, etc. are due to the sludge [7].

The addition of 2% copper nitrate caused the appearance of a 0.649 nm peak, the strongest peak in the pattern. This peak was associated with $CuO \cdot 3H2O$ (PDF# 36,0545) [8]. Several peaks of this phase could be found in the pattern. The 0.262 nm peak is the strongest peak of the $CuO \cdot 3H2O$ phase. This is also the strongest peak of CH. As no other peak of CH was present, no CH was identified in the 2% copper nitrate

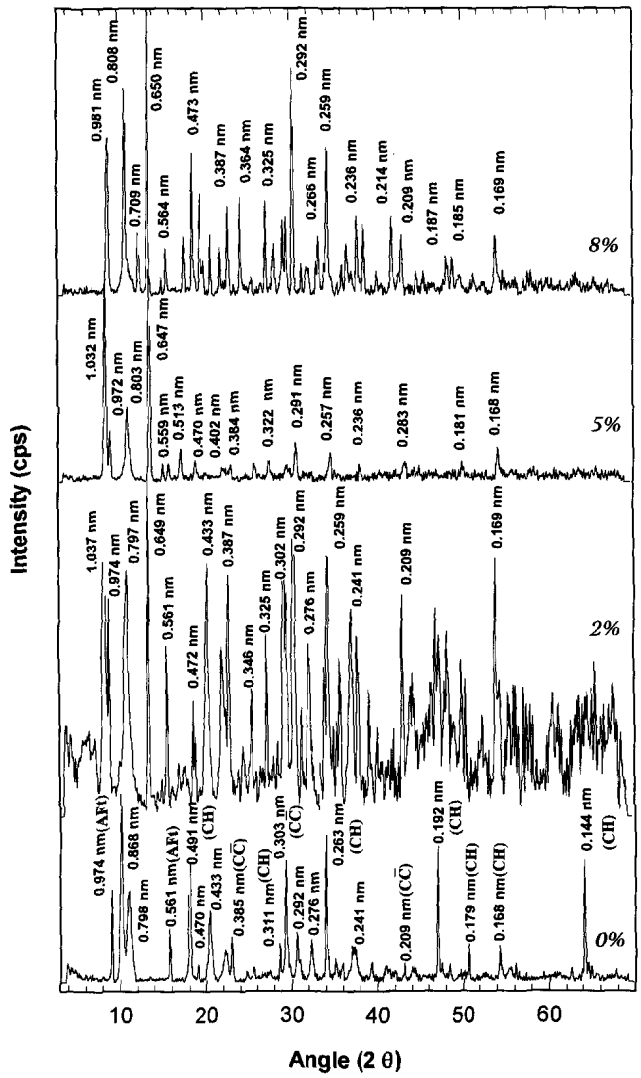

Fig. 8. XRD patterns of OPC–sludge–copper nitrate waste form. The patterns are background and $K\alpha_2$ subtracted runs.

containing waste form. Several peaks of the sludge, found in the control pattern, could be identified in the sample (Table 3). AFt and CC^- were also present.

Fewer AFt peaks were present when 5% copper nitrate was added. Some amount of CC^- was also detected. Several of the sludge peaks were also present in the pattern, whereas a few others disappeared, for example, the 0.798 nm peak. The 0.647 nm peak continued to be the most intense peak in the pattern.

The 8% copper nitrate waste form pattern had a significantly greater number of peaks

Table 3
FTIR peaks in sludge and OPC–sludge–copper nitrate waste form

Sludge (cm^{-1})	OPC (cm^{-1})	Observation	Comments
	3615	5% and 8%	OH
3430	3491–543	All	ν_1 and ν_2 from H_2O
2512	2517		
2426	2467	↑ to 5%	
	2395	↑ to 5%	
1795	1797	↑ to 5%	NO_3^{2-}, CO_3
1636	1634	↑ to 8%	δ HOH from H_2O
1429	1427	↑ broad	CO_3 in calcite
1385	1385	↑ broad	OH [a]
1048	1048	Only in 8%	ν_1 from NO_3^{2-}
	975–980	↓ to 8%	Si–O in C–S–H; sharpness increases to 8%.
874	874	↓ to 8%	calcite
822	821	From 2% up	ν_2 from NO_3^{2-}
	784	↓ to 8%	
713			
	603	Only in 8%	
514			
	513	5% and 8%	Si–O, ν_3; sharpness increases to 8%.
	454	0% and 2%	OH

↑ ↓: Increasing or decreasing intensity.
[a] Assigned to metal–OH bond [9].

than the other samples. The sludge peaks also appeared to be more intense compared to the samples with lesser levels of copper nitrate. This could be due to two reasons: there were new crystalline phases and/or the crystallinity of the phases already present increased. The 0.650 nm peak was the most dominant peak in the pattern. The 0.981 and 0.654 nm peaks could correspond to the 0.973 nm (100% relative intensity) and 0.561 nm (80% relative intensity), respectively, peaks of AFt (PDF# 9,414) [8]. But other AFt peaks of high relative intensities were absent, suggesting that AFt was absent in this sample.

With the increasing amount of copper nitrate some of the sludge peaks remained unaffected (such as 0.292, 0.473 and 0.399 nm), but others, such as the 0.798 and 0.433 nm peaks were absent from the 5% copper nitrate sample onward. Table 3 shows that peaks in the low 2θ region of the patterns could not be precisely matched. This is not surprising as these peaks were due to impure phases, and also the errors in d-spacing calculations are higher at the 2θ region. Extensive computer search-match of the XRD patterns of the copper nitrate containing waste forms with the JCPDS [8] did not produce any perfect match of the peaks with pure phases in the JCPDS. Several peaks from the 2% pattern onward could be matched (Table 3) with the peaks for $CuO \cdot 3H_2O$ (PDF# 36,0545), but the relative intensities could not be matched. For example, the PDF file lists 20% relative intensity for the 0.650 nm peak (-101 plane) and 100% relative intensity for the 0.263 nm (005 plane) peak. The 2% pattern had 100% relative intensity for the 0.650 nm peak and 20% for the 0.263 nm peak. The 0.262 nm peak was absent from 5% copper nitrate concentration upward.

3.2.4. Thermal analysis

3.2.4.1. Differential scanning calorimetry. Fig. 1 shows the DSC curves of OPC and the waste form containing various amounts of copper nitrate. The breakdown of CH in OPC occurred over a temperature range extending beyond the 525°C limit of the run. The 53–55°C peak was present only in the 0% and 2% samples. A comparison of the OPC and the sludge- and copper nitrate-containing waste forms suggests that the 99–95°C peak corresponded to the same phase, whereas the 117°C peak in the 8% sample was from a new phase. The 285°C peak in the 0% copper nitrate waste form could be the 272°C sludge peak, but the higher temperature (323°C) sludge peak was absent in the 0% and 2% copper nitrate containing waste form. Instead, there was a new peak in the 414 to 392°C region. For the 5% sample, the derivative of the DSC curve shows that that were at least three peaks in the 200 to 400°C range. The 200 to 400°C region of the sludge and 8% copper nitrate waste forms appeared somewhat similar. The 449°C peak could be due to a new phase or grew more intense from the 392 (2%) through 437°C (5%) peak. If the latter argument is true, then a small amount of this phase formed in the 2% sample, then increased more and more through 5% and 8%.

3.2.4.2. Thermogravimetry. Thermogravimetry showed that the 5% copper nitrate containing waste form lost up to 60% of its starting mass at 1000°C, whereas at 8% copper nitrate level the loss was about 54%. The mass loss for the OPC, hydrated at the same water/solids ratio (2.5), was 54%.

3.2.4.3. Derivative thermogravimetry. The DTG curves of the waste form with increasing amounts of copper nitrate, along with those of OPC and the sludge, are shown in Fig. 2. A comparison of the OPC and the 0% copper nitrate waste form shows that the peaks at 276 and 376°C were due to the sludge. The AFt peak was well-resolved and the amount of AFt was higher compared to the OPC. The 651°C peak was due to CC^{-}. The amount of CC^{-} was 3.1%.

AFt (84°C) was still detected when 2% copper nitrate was present. The region 200 to 500°C consisted of three peaks which appeared to be the same as those in the 0% copper nitrate sample, but with the 376°C peak highly diminished. This peak was present as a weak left shoulder of the 442°C peak. The significant reduction of the 376°C peak compared to no reduction of the 272°C peak suggests that these two peaks were due to two different phases. The 625°C peak was from CC^{-}, the amount being 1.4%. A new peak appeared in this sample at 809°C.

When 5% copper nitrate was added, further changes were observed. There was a tall peak at 69°C. This could be the same peak seen at slightly lower temperature in the 0% (67°C) and 2% (49°C) waste forms. No separate AFt peak was identified, suggesting that AFt was absent in this sample. The 272°C peak was unaffected, the 376°C peak was completely absent and a larger peak was present at 468°C. The 468°C peak was not due to CH as the peak temperature for pure CH runs never occurred beyond 435°C under the run conditions used in this study. The 617°C peak corresponded to CC^{-} (1.3%). The 834°C peak was due to the same phase as the 809°C peak in the 2% sample, but was present in higher concentration.

The addition of 8% copper nitrate to the waste form brought more changes. Both the 69°C peak present in the earlier sample and AFt were absent in this sample. Several new peaks appeared in this sample: at 95, 231 and 294°C. The 272°C peak shifted to 262°C, presumably being less in proportion. The left shoulder of the peak at 453°C showed an unresolved peak. The 643°C peak is from CC^- (3.6%). The 861°C peak was due to the same phase as seen in the 809–834°C region in the 2% and 5% samples. The amount of this phase increased with increasing copper nitrate concentration.

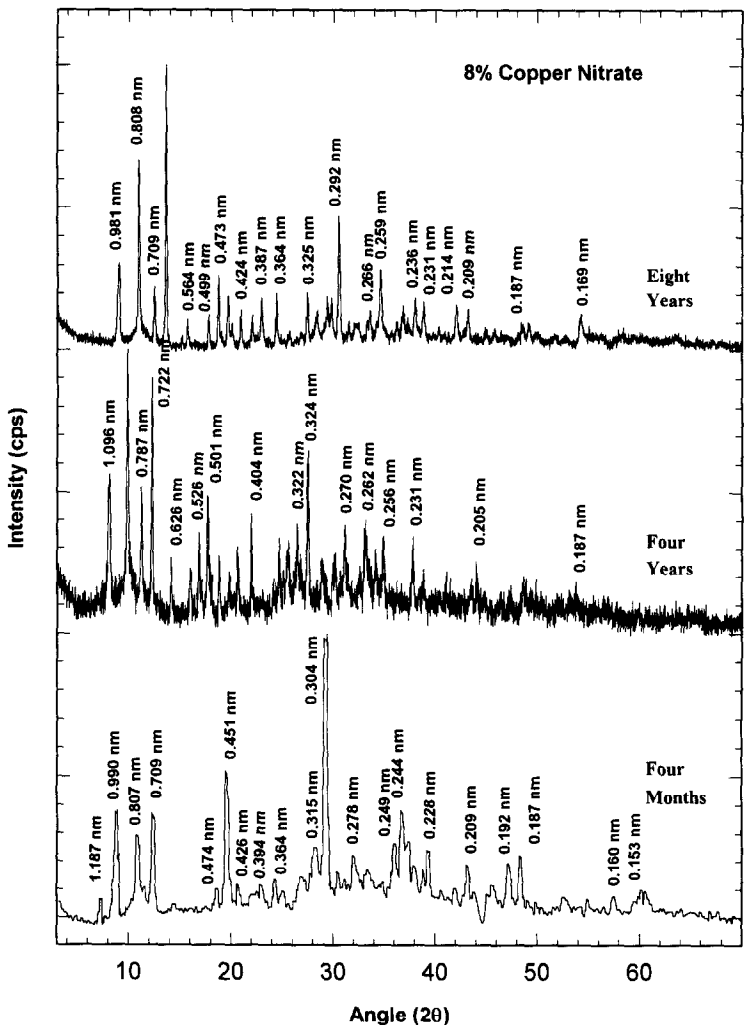

Fig. 9. XRD patterns of OPC–sludge waste form with 8% copper nitrate over time. The patterns are runs without any data treatment.

3.2.5. Fourier-transform infrared spectroscopy

The FTIR spectra of the waste form with increasing amounts of copper nitrate are shown in Fig. 3 and the peaks are tabulated in Table 2. Distinct trends were present in the FTIR spectra with increasing interferent concentration. For example, the 1633 cm^{-1} peak for H_2O became more intense with increasing interferent concentration. Some

Table 4
XRD peaks in 8% copper ntiate OPC–sludge wasteform over 8 years (in nm)

4-Months	4-Years	8-Years	Comments	4-months	4-years	8-years	Comments
1.187							
1.044	1.096			0.319			
0.990				0.315			
	0.898			0.310	0.309		$CuO \cdot 3H_2O$
		0.981		0.304		0.304	CC^-
0.807		0.808				0.300	
0.780	0.787					0.300	
0.760						0.292	Sludge
0.739						0.283	
0.709		0.709		0.278			
	0.722	0.650	$CuO \cdot 3H_2O$	0.276		0.277	$CuO \cdot 3H_2O$
	0.626			0.275			
		0.584			0.270	0.269	
		0.564		0.267		0.266	
					0.262		$CuO \cdot 3H_2O$
	0.553					0.259	
	0.526				0.256		$CuO \cdot 3H_2O$
	0.501	0.499		0.247			
0.474	0.471	0.473	Sludge; $CuO \cdot H_2O$			0.244	
0.451	0.448	0.451		0.240			
0.443		0.442		0.238	0.238		
	0.430			0.236		0.236	$CuO \cdot 3H_2O$
0.426		0.424	$CuO \cdot 3H_2O$	0.231			
0.426		0.424	$CuO \cdot 3H_2O$	0.231			CC^-
0.403	0.404	0.403		0.228			
0.397				0.209			
0.394					0.205		
		0.387	CC^-			0.197	$CuO \cdot 3H_2O$
0.364		0.364	$CuO \cdot 3H_2O$	0.198			CC^-
	0.360			0.192			CC^-
	0.348			0.191			CC^-
	0.337			0.187	0.187	0.187	CC^-
0.331	0.332					0.182	
0.329				0.173	0.176		
0.326	0.324	0.325				0.169	$CuO \cdot 3H_2O$
						0.166	
		0.314					$CuO \cdot 3H_2O$
				0.154			
				0.152			
						0.146	
				0.143			

peaks were found only when copper nitrate was added, for example, the 821 cm^{-1} peak. The 1427 cm^{-1} peak became less sharp and broader with increasing copper nitrate concentration. The carbonate and nitrate peaks have vibrations of similar magnitudes because of their similar molecular characteristics [10] and thus can have overlapping peaks. The presence of both of these may have broadened the 1427 cm^{-1} peak. Some peaks, such as 784 cm^{-1}, disappeared with increasing interferent concentration. The 975 cm^{-1} C–S–H peak in the OPC–sludge waste form shifted to 980 cm^{-1} with the addition of 2% copper nitrate; however, further addition of copper nitrate did not affect the position of this peak. The 513 cm^{-1} silicate peak, which appeared in the 5% sample, also became sharper with increasing copper nitrate addition.

3.3. Long-term behavior

Scanning electron microscopy showed that the same morphologies identified in the four-month old waste form were present in the eight-year old waste form. For example, Fig. 4 is a photomicrograph of the 8% copper nitrate OPC–sludge waste form at four months of age.

Fig. 9 shows the XRD patterns of the 8% copper nitrate containing waste form and Table 4 lists the XRD peaks in the four-month old waste form, when it was 4 years old, and at 8 years. There is remarkable similarity between the four-month old pattern and the eight-year old pattern, except the $CuO \cdot 3H_2O$ peaks. Peaks for this phase were not present in the 4-month old samples at any concentration of copper nitrate. The peaks for the hydrated copper oxide phase were identified in the 4-year old 2% and 5% copper nitrate containing waste form, but were absent from the 8% copper nitrate containing waste form. Some other changes were also observed. For example, CH was identified in the 4-year old 2% copper nitrate containing waste form, but it was absent in the 8 year old sample having the same copper nitrate concentration. CC^{-} peaks were very intense in the 4-month old samples. This could be due to a higher fraction of the sample coming from the carbonated surface of the sample. Fewer matches between the 4-year old sample and the 4-month and 8-year old samples could be due to sample inhomogeneity.

DTG of the waste form over a 14-month period to the present did not show any differences. These various lines of evidence thus suggest that practically the same chemical species were present from 4 months onward.

4. Discussion

Several analytical techniques are usually required for unambiguous identification of the chemical species present in solidified/stabilized waste forms. Unlike XRD, the peak breakdown temperatures in the DTG curve of a material do not reflect fundamental properties of a phase(s) in a material. The peak temperatures depend on several factors, such as heating rate, configuration of the instrument, material of the sample pan, purge gas flow rate, etc. [11]. However, in conjunction with other material characterization techniques, DTG can provide important constraints in identifying and quantifying unknown materials, particularly hydrated and carbonated phases.

FTIR provided some important evidence on the composition of the phases in the waste form. The 1630 cm^{-1} peak became stronger with increasing copper nitrate concentration suggesting molecular water was an important constituent of the chemical species in the waste form. The peak position also suggested that this molecular water was weakly held, similar to the clay mineral montmorillonite [12]. The 1385 cm^{-1} OH peak became weaker with increasing copper nitrate concentration. FTIR showed that most of the carbonate was present as calcite.

Thermogravimetry of the waste form indicated that up to 60% of its mass was lost when samples were heated up to 1000°C. Molecular water and hydroxyl ions in hydrated phases and carbon dioxide from carbonates are usually lost in this temperature range. (Sulfates and nitrates may also break down in this temperature range, but there is very little sulfate to begin with in the waste form studied.) Along with FTIR evidence, this mass-loss then indicates the presence of molecular water and hydroxyl molecules in the phases present in the waste form.

In this study, SEM indicated that at the 8% copper nitrate level the bulk of the matrix (C–S–H) of the waste form was very different from the 0% level. In the 8% copper nitrate containing waste form, a significant portion of the matrix was composed of tabular crystals with well-defined faces. Though XRD showed $CuO \cdot 3H_3O$ was an important phase in the presence of copper nitrate, EDXRA did not indicate that any of the larger crystalline phases contained Cu as the only cation. However, the maximum amount of copper nitrate was 8 wt%, and thus on a weight basis it was minor and could not constitute the bulk of the matrix.

4.1. Waste chemical species in waste form

4.1.1. Copper-bearing phases

Patterson et al. [13] reviewed the copper nitrate precipitation process by alkalies and conducted additional experiments on the process. The initial product of copper nitrate and NaOH reaction is a colloidal metastable copper hydroxide which on aging converts to more stable, slightly hydrated, copper oxide. The colloidal precipitate contains ca. 20 mol of water for 1 mol of copper. The exact nature of the precipitate depends on the addition rate of the reactants and even on the order of addition.

In the present study, XRD did not indicate that CuO was present in the waste form at any copper nitrate concentration. A copper hydrate phase, $CuO \cdot 3H_2O$, was identified in the waste form in the presence of copper nitrate. $CuO \cdot 3H_2O$ phase was synthesized by Sen Gupta et al. [14] as a higher temperature (265°C) breakdown product of a copper–urea complex. The lack of good correspondence between the $CuO \cdot 3H_2O$ XRD pattern reported in the literature and those obtained in the present study could be due to several reasons. Orientation of anisotropic crystals along a preferred direction is a common occurrence during sample preparation for XRD. This frequently happens for clay minerals and CH, both of which have a platy habit, and results in relative intensities different from those reported in the PDF files. Poor crystallinity may also account for this mismatch. The $CuO \cdot 3H_2O$ phase [14] was synthesized at much higher temperature than the ambient temperature of this study. At room temperature, this phase may have low crystallinity. In addition, EDXRA and SEM did not show the presence of larger

(greater than a micrometer) crystals with copper as the principal cation. It is possible that the hydrated copper oxide phase is present as sub-micrometer-size crystallites.

According to the reported equilibrium constants, air-saturated water will favor precipitation of $CuO_{(solid)}$ over the whole pH range when Cu^{2+} ions are present [15]. Azurite ($Cu_3(CO_3)_2(OH)_2$) or malachite ($Cu_2(CO_3)(OH)_2$) can precipitate at lower pH [16] when carbon dioxide activity is higher than in air–saturated water. In the absence of copper nitrate, the pH of the waste form studied was buffered by CH (12.5), but increasing the amount of copper nitrate added pushed the pH of the system below 11.6–11.4 (as noted by the absence of AFt in the 8% copper nitrate sample). Azurite and malachite can thus potentially form in the waste form studied. XRD did not show any match between the patterns of the waste forms obtained in this study and those in the PDF files of azurite or malachite. The broad carbonate FTIR peak in the 1500 to 1400 cm^{-1} region of azurite and malachite is split into several sub-peaks, whereas calcite has a single peak in the region [17]. The FTIR patterns of the waste form with increasing amount of copper nitrate showed only peaks corresponding to calcite, suggesting that it is the principal form of carbonate present. Thus both XRD and FTIR suggest that azurite or malachite are absent in the OPC–sludge–copper nitrate waste form.

4.1.2. Other phases

A peak in the region 800 to 700°C appeared when copper nitrate was first added to the waste form. The peak shifted to higher temperatures with increasing copper nitrate concentration, suggesting a proportionate increase in the amount of this phase in the waste form. This peak may be due to the breakdown of the nitrate phase, the chemical speciation of which was not identified.

4.2. Effects of copper nitrate on the S / S process

Jones et al. [4] determined the leaching behavior of this waste form by EP toxicity test. Little change in phase composition of the waste form over eight years suggests that the present composition can be used to interpret the pH measurements conducted on 28-day old samples. They observed a systematic decrease in the pH of the final leachate with increasing copper nitrate concentration. The pHs were basic even after adjustment during the 24 h test. The pH dropped from 11.5 for the 0% sample to 10.3 for the 8% sample. The continuous drop in pH suggests absence of any buffering phase such as CH or AFt. Indeed, XRD indicates that CH was absent in the presence of copper nitrate, and the 8% sample had no AFt which could have buffered the pH around 11.6–11.4 [18].

Earlier work [7] and the present investigation have shown that the heavy metal sludge consists of impure, complex hydroxides and hydrated phases. The addition of copper nitrate to the waste form led to the disappearance of some of these phases, whereas others remained unaffected. For example, in the XRD patterns some of the sludge peaks could be traced through all samples, irrespective of copper nitrate concentration, suggesting that the interferent had no effect on the sludge. Similarly, sludge peaks in the DTG or DSC patterns could be traced through all samples, irrespective of copper nitrate level. The dissolution of some of the sludge phases then may lead to increased leaching of the elements present in these phases. Jones et al. [4] measured the heavy metal

concentration in the leachate generated from the waste form by the EP toxicity procedure. The leachate concentration of Cr, Ni and Cd increased with decreasing pH, i.e., increasing copper nitrate concentration. The XRD pattern of the waste forms containing 8% copper nitrate had several of the sludge peaks intensified compared to the control or other patterns (Fig. 8). During sample preparation, the OPC–sludge waste form was divided into 4 parts, and 0%, 2%, 5% or 8% copper nitrate was added to each part. Since many of the heavy metal reactions are kinetically controlled and depend on the amount and the order in which a reactant is added, the effect of differing amounts of copper nitrate may be different on the same OPC–sludge waste form.

OPC containing copper nitrate has been studied [19]. However, the amount of copper nitrate in the system was 1000 ppm for 10 g of cement (w/c = 0.4). Their reported XRD pattern showed that CH was present in appreciable amount. This is not surprising, as the amount of copper nitrate is not adequate to neutralize all the CH in the system. The waste form studied here had a lower initial amount of CH due to retardation of the cement reactions by the sludge, and the remaining CH was neutralized by the added copper nitrate.

SEM suggested, qualitatively, that the porosity of the waste form increased with increasing amount of copper nitrate. This may lead to increased leaching. Some amounts of copper and chromium are also trapped in the crystalline calcium silicate phases. The leachability of these elements will depend on the solubility of these phases.

4.2.1. C–S–H

SEM and EDXRA observations suggested that the crystallinity of the cement matrix was strongly affected by copper nitrate. Newer crystalline morphologies were observed in the waste form even when 2% copper nitrate was added. At 5% copper nitrate level, abundant fibrous crystals were observed; at 8% level, tabular crystals with tapering faces were observed. EDXRA showed that these crystals were calcium silicates with minor amounts of copper. The poorly crystalline C–S–H in OPC became more crystalline with increasing amounts of copper nitrate. (The exact morphology of these crystalline phases is not important as the presence of foreign ions often poisons crystals and can make crystals grow in different ways.)

FTIR also corroborates this observation. The C–S–H peak shifted to 975 to 980 cm^{-1} with the addition of 2% copper nitrate but remained unchanged with the further addition of copper nitrate. This peak and the 513 cm^{-1} peak became sharper with a further increase in copper nitrate concentration. The sharpness of an FTIR peak depends on the crystallinity of the phase, the peak for the amorphous phase being broader than the crystalline phase. The shift of the SiO_4^{2-} vibration to a higher wave number and increasing sharpness of the peak suggest that the silicate phase became more polymerized and more crystalline.

4.2.2. Carbonation

Some amount of carbonation was present in the waste form at all copper nitrate levels, the average amount being 4.0%. The highest amount of CC^- was present in OPC, 4.3%. The high w/c ratio (2.5) and the subsequent high porosity would make this amount of carbonation reasonable. In addition to the OPC component, the CH in the

sludge is also susceptible to carbonation, which would increase the amount of CC^- in the OPC–sludge waste form.

4.3. Long-term behavior

The principal copper-bearing phase in the waste form with copper nitrate is metastable $CuO \cdot 3H_2O$, compared to more stable CuO. The heavy metals in the sludge are also present as impure complex hydroxides and hydrated phases rather than as simple hydroxides. Analytical evidence shows that, over the long term, at the same copper nitrate level, there have been subtle changes in the waste form chemistry since its preparation. The hydrated copper oxide phase was not present at 4 months but appeared by four years at 5% and 8% copper nitrate level, and by 8 years also at 8% copper nitrate level. Similarly, CH was still identified at the 2% copper nitrate level in the 4-year old waste form, but it was completely consumed in the 8-year old waste form at the same copper nitrate level. The process of $CuO \cdot 3H_2O$ crystallization is thus slow, as discussed by Patterson et al. [12]. The sludge phases, however, remained unchanged.

5. Conclusions

S/S of the heavy metal sludge in the presence of copper nitrate is a complex process. Some phase(s) in the heavy metal sludge remained unaffected by the addition of copper nitrate to the waste form whereas other(s) dissolved. The presence of the interfering compound, copper nitrate, affected the sludge species by reducing the pH of the waste form. The pH of the waste form decreased with increasing copper nitrate concentration and with time, as evidenced by the gradual disappearance of CH and AFt.

Subtle changes in the microchemistry of the waste form occurred over time. The appearance of $CuO \cdot 3H_2O$ was concentration dependent. This phase was absent in the four-month old waste form with any concentration of copper nitrate; it was present in the 4-year old waste form at copper nitrate concentration of up to 5%; in the 8-year old waste form it was present at all concentrations of copper nitrate. CH was slowly consumed over time. It was present in the 4-year old waste form with 2% copper nitrate, but was absent in the 8-year old waste form. The addition of copper nitrate increased the crystallinity and porosity of the matrix. There was very little visible change in the microstructure of the waste form from four months onward.

References

[1] J.R. Conner, Chemical Fixation and Solidification of Hazardous Wastes (Van Nostrand Reinhold, New York, 1990) pp. 692.
[2] K.L. Perry, N.E. Prange and W.F. Garvey, ASTM STP 1123 (1992) 242.
[3] H. Akhter and F.K. Cartledge, Div. Environ. Chem., 202nd Natl. Meet., Am. Chem. Soc., New York, NY, August 1991.
[4] L.W. Jones, R.M. Bricka and M.J. Cullinane, Jr., ASTM STP 1123 (1992) 193.
[5] J.M. Cullinane, R.M. Bricka and N.R. Francingues, 13th Annu. EPA RES. Symp., Cincinnati, OH, 1987, p. 64.

[6] T. Taylor Eighmy, J. Dykstra Eusden, Jr., J.E. Krzanowski, D.S. Domingo, Dominique Stampfli, J.R. Martin and P.M. Erickson, Environ. Sci. Technol. 29 (1995) 629.
[7] A. Roy, H.C. Eaton, F.K. Cartledge and M.E. Tittlebaum, Environ. Sci. Technol. 26 (1992) 1349.
[8] Joint Committee for Powder Diffraction Standards, Powder Diffraction File, International Center for Diffraction Data, Swarthmore, PA, 1992.
[9] H.A. Szymanski, Infrared Band Handbook (Plenum, New York, 1970) pp. 1491.
[10] K. Nakamoto, Infrared Spectra of Inorganic and Coordination Compounds (Wiley, 1970, New York) pp. 338.
[11] W.Wm. Wendlandt, Thermal Analysis, 3rd Ed. (Wiley, New York, 1986) pp. 814.
[12] H.W. van der Marel and H. Beutelspacher, Atlas of Infrared Spectroscopy of Clay Minerals and Their Admixtures (Elsevier, Amsterdam, 1976) pp. 396.
[13] J.W. Patterson, R.E Boice, C. Petropoulu, D. Marani, D. Macchi and G. Macchi, Hydrolysis, In: J.W. Patterson and R. Passino (Ed.), Metals Speciation, Separation, and Recovery (Lewis, Chelsea, MI, 1990) p. 169.
[14] A. Sen Gupta, P.C Srivatsava, C. Aravindakshan and B.K. Banerjee, J. Phys. Chem. Solids 43 (1982) 645.
[15] C.F. Baes, C.F., Jr. and R.E. Mesmer, The Hydrolysis of Cations (Wiley, New York, 1976) pp. 489.
[16] W. Stumm and J.J Morgan, Aquatic Chemistry, 2nd Edn., (Wiley, New York, 1981) pp. 780.
[17] C.W. Jones and B. Jackson, Infrared Transmission Spectra of Carbonate Minerals (Chapman and Hall, London, 1993).
[18] M. Atkins, D. Macphee, A. Kindness and F.P. Glasser, Chem. Conc. Res. 21 (1991) 991.
[19] T.-T. Lin, C.-F. Lin, W.-C.J. Wel and S.-L. Lo, Environ. Sci. Technol. 27 (1993) 1312.